3.2Gbps Channel-Adaptive Configurable MIMO Detector for Multi-Mode Wireless Communication

Farhana Sheikh, Chia-Hsiang Chen, Dongmin Yoon, Borislav Alexandrov, Keith Bowman, [*]Anthony Chun, Hossein Alavi, [†]Zhengya Zhang

Intel Labs, Hillsboro, OR USA; [*]Intel Labs, Santa Clara, CA USA; [†]Dept. of EECS, University of Michigan, Ann Arbor, MI
E-mail: farhana.sheikh@intel.com

Abstract—**A configurable, channel-adaptive K-best MIMO detector for multi-mode wireless communications that adapts computation to varying channel conditions to achieve high energy-efficiency is presented. An 8-stage configurable MIMO detector supporting up to a 4x4 MIMO array and BPSK to 16-QAM modulation schemes has been implemented and simulated in 0.80V, 22nm Tri-gate CMOS process. Dynamic clock gating and power gating enable on-the-fly configuration and adaptive tuning of search radius K to channel response which results in 10% to 51% energy-efficiency improvement over non-adaptive K-best MIMO detectors. During unfavorable channel conditions, the MIMO detector satisfies target BER by setting K=5. For favorable channel conditions, K is reduced to 1, where 22nm circuit simulations show 68% energy reduction. At 1.0GHz target frequency, the total power consumption is 15mW (K=1) to 35mW (K=5), resulting in energy-efficiency of 14.2pJ/bit (K=1) to 44.7pJ/bit (K=5) and 3.2Gbps throughput.**

Keywords—Multiple Input, Multiple Output (MIMO) detector; channel-adaptive; LTE systems; IEEE 802.11n/ac; K-best; sphere decoding; multi-mode communication; reconfigurable.

I. INTRODUCTION

New advanced wireless communication standards such as IEEE 802.11n/ac and 3GPP LTE Advanced Release 10/11 take advantage of a multiple-input, multiple-output (MIMO) communication schemes to enable increased spectral efficiency and high throughput data rates. For example, IEEE 802.11n allows for up to 4x4 antenna array (up to 4 streams with 4 transmit and 4 receive antennas); IEEE 802.11ac calls for up to an 8x4 array (8 AP and 4 STA antennas) and 3GPP LTE Advanced release 10 [1] specifies up to an 8x8 antenna array. The enhancement in spectral efficiency and higher throughput comes at significant computational cost: work load profiling indicates that MIMO detection at the receiver can consume up to 42% of the compute cycles in the physical layer baseband processing. The goal of this work is to present a configurable MIMO detector that can support multiple standards and adapt its computation to different channel conditions to improve energy-efficiency and reduce computational complexity.

A MIMO detector is used to determine the most likely data sequence transmitted by combining the multiple input streams at the receiver (see Fig. 1). There are a number of different algorithms used for MIMO detection as summarized in Table 1. Optimal Maximum Likelihood (ML) detection theoretically achieves the minimum bit-error rate (BER) but it is also the most expensive to implement since its complexity grows exponentially with increasing number of antennas, resulting in large area and power requirements.

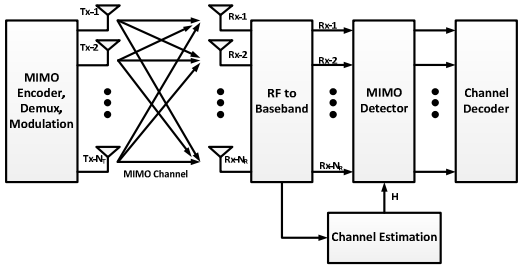

Figure 1. MIMO system overview

In order to achieve high BER at reduced computational complexity, the sphere decoding (SD) algorithm [2] is used to achieve near-ML detection performance by examining only a subset of solutions within a specified search radius [3]. Theoretically, the SD algorithm has cubic computational complexity with respect to the number of antennas. Two types of algorithms are used to traverse the search space: depth-first search [9] and K-best breadth-first search [2]. In this work, we focus on K-best breadth-first search which enables regularized datapath interconnect and parallelism. The rest of this paper is organized as follows. Section II reviews different MIMO detection algorithms, the SD algorithm, and advantages/disadvantages of different search criteria. Section III presents a summary of prior publications in this area. Section IV and Section V detail the design and implementation of the channel-adaptive reconfigurable K-best MIMO detector. Section VI presents simulation results in 22nm CMOS and Section VII concludes the paper.

II. MIMO SYSTEMS AND DESIGN CHALLENGES

Figure 1 shows the system architecture for a generic MIMO system. At the transmitter, a coded data stream is de-multiplexed onto N_t antennas. The data streams may be modulated using different constellation sets of quadrature amplitude modulation (QAM) symbols. The use of multiple transmit channels allows the MIMO system to maximally use limited spectrum and deliver data at very high rates. At the receiver, the signals are processed by the analog front-end into I and Q streams for each received signal at each antenna. The digital front-end (DFE) performs carrier frequency offset compensation, synchronization, and equalization. The MIMO detector combines each of the

complex received signals at the receiver before further processing in the channel decoder.

As antenna arrays increase to 8x8 and higher to meet increasing performance requirements, the complexity of MIMO detection in the physical downlink baseband processing grows exponentially, taking up to 42% of compute cycles which results in large area and power. The ideal MIMO detector has low area/power costs but is able to provide consistent required BER performance based on application needs in different types of channel conditions and for different wireless standards.

A. MIMO System Model

A MIMO system with N_t transmit antennas and N_r receive antennas, operating in a symmetric M-QAM scheme, with $\log_2 M$ bits per symbol is modeled by:

$$\boldsymbol{y} = \boldsymbol{H}\boldsymbol{s} + \boldsymbol{v}, \tag{1}$$

where $\boldsymbol{s} = \left[s_1, s_2, \dots s_{N_t}\right]^T$, $(s_i \in \mathcal{S})$ is the N_t-dimensional complex information symbol vector transmitted. The set $\mathcal{S}$ is the constellation set of the QAM symbols, and $\boldsymbol{y} = \left[y_1, y_2, \dots, y_{N_r}\right]^T$ is the N_r-dimensional complex information symbol vector received. The equivalent baseband model of the Rayleigh fading channel between the transmitter and receiver is described by a complex valued $N_r \times N_t$ channel matrix $\boldsymbol{H}$. The vector $\boldsymbol{v} = \left[v_1, v_2, \dots, v_{N_r}\right]^T$ represents the N_r-dimensional complex zero-mean Gaussian noise vector with variance σ^2 [4].

The ML detector estimates the transmitted signal by solving:

$$\hat{\boldsymbol{s}} = \arg\min_{\tilde{\boldsymbol{s}} \in \mathcal{S}^{N_t}} \|\boldsymbol{y} - \boldsymbol{H}\tilde{\boldsymbol{s}}\|^2, \tag{2}$$

where $\tilde{\boldsymbol{s}}$ represents the candidate complex information symbol vector and $\hat{\boldsymbol{s}}$ is the estimated transmitted symbol vector. Eq. (2) is generally non-deterministic polynomial hard (NP-hard) and represents the closest point problem [5] which is a search through the set of all possible lattice points for the global best in terms of distance between the received signal $\boldsymbol{y}$ and $\boldsymbol{H}\tilde{\boldsymbol{s}}$. Effectively, Eq. (2) describes a tree search problem where each of the constellation points in $\mathcal{S}^{N_t}$ are evaluated to find the path through the tree that minimizes the global error. The goal is to find the closest vector $\tilde{\boldsymbol{s}}$ to the original transmitted symbol vector $\boldsymbol{s}$ given vector $\boldsymbol{y}$.

The channel matrix $\boldsymbol{H}$ can be factored into two simpler matrices using QR factorization, where $\boldsymbol{Q}$ is a $(N_r + N_t) \times N_t$ orthonormal unitary matrix and $\boldsymbol{R}$ is a $N_t \times N_t$ upper triangular matrix such that $\boldsymbol{H} = \boldsymbol{Q}\boldsymbol{R}$. Eq. (2) is then reformulated as:

$$\hat{\boldsymbol{s}} = \arg\min_{\tilde{\boldsymbol{s}} \in \mathcal{S}^{N_t}} \|\tilde{\boldsymbol{y}} - \boldsymbol{R}\tilde{\boldsymbol{s}}\|^2, \tag{3}$$

where $\tilde{\boldsymbol{y}} = \boldsymbol{Q}^T\boldsymbol{y}$. The diagonal elements of $\boldsymbol{R}$ are real and since it is upper triangular, symbol detection begins from the last row (i.e. top node in the tree) and moves up through the matrix in several steps until the unknowns in the first row (i.e. last level in the tree) are determined [3]. Several non-optimal and near-optimal algorithms have been proposed in the literature to traverse the search space to determine $\hat{\boldsymbol{s}}$ such that the total error is minimized. They are summarized in the next section and in Table 1.

Table 1. MIMO detection algorithm tradeoffs

Detector Type	BER Performance	Computational Complexity	In a Large MIMO System
Optimal Detectors • Maximum Likelihood (ML) • Sphere decoder (SD)	Optimal	Exponential	Heavy computation (prohibitively high area/power)
Sub-optimal detectors • Zero Forcing (ZF) • Minimum Mean Square Error (MMSE) • V-BLAST • Successive Interference Cancellation (SIC)	Poor	Linear, Polynomial	Inaccurate (error propagation)
Near-ML detectors • SD with termination criteria • K-best SD, LR-aided • Markov Chain Monte Carlo	Near optimal	Polynomial	Feasible (potentially high power/area)

B. MIMO Detection Algorithms

Several algorithms have been proposed to address the complexity of MIMO detection in the receiver, offering different tradeoffs between power and performance. Table 1 gives an overview of MIMO detection techniques and qualitative tradeoffs. Among the MIMO detection techniques listed in Table 1 and shown in Fig. 2, the ML detector minimizes the BER performance through exhaustive search, but complexity grows exponentially with increasing number of antennas [3]. In contrast, linear detectors (LDs) – such as zero-forcing and MMSE detectors – and successive interference cancellation (SIC) detectors that have polynomial complexity suffer from significantly higher BER for the same signal-to-noise ratio (SNR). Markov Chain Monte Carlo methods [6] perform well in low SNR channel conditions but exhibit poor performance in high SNR channels. The SD detector using depth-first search without termination criteria results in optimal BER as in the case of a ML detector but requires prohibitively large area and power, and may never reach its solution in bounded time. Sphere decoding using breadth-first search with termination criteria can achieve near-optimal performance with polynomial computational complexity; however, such detectors may still require high area/power as antenna arrays increase. In this work, we focus our implementation on SD detection with breadth-first search and limit the number of candidates evaluated in each step to $\boldsymbol{K}$ candidates with minimum partial distance from $\tilde{\boldsymbol{y}}$. The next section details the K-Best SD detection algorithm with termination criteria.

C. K-Best Sphere Decoding with Termination Criteria

The main advantage of depth-first search is that ML performance can be achieved and radius shrinking can be used to prune the search. The advantages of the K-Best breadth-first search over the depth-first search is the regular

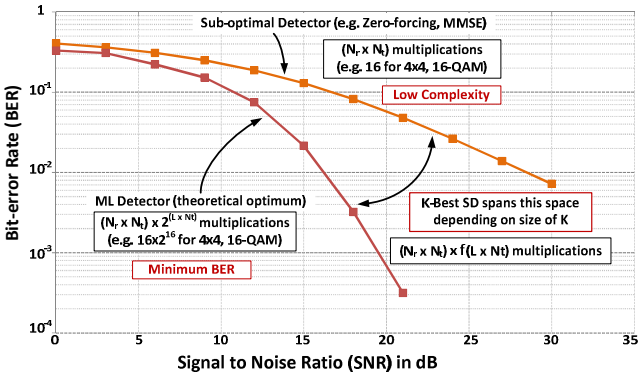

Figure 2. MIMO detection algorithm tradeoffs

datapath interconnect and potential for parallelization to improve throughput. The K-Best tree search for MIMO [2] is a particular subset of breadth-first tree search algorithms.

It represents a middle ground between the complexity of the ML detector and linear detectors, finding a better sub-optimal solution to the closest point search than the linear detectors, with less complexity than the ML detector as shown in Fig. 2. The K-Best SD solution can span the BER vs. SNR tradeoff space by adjusting $\boldsymbol{K}$ based on application BER requirements and channel conditions. In this work, we take advantage of this property to enable a configurable detector that behaves as a linear detector when channel SNR is high by setting $\boldsymbol{K} = \boldsymbol{1}$ and when SNR is low, $\boldsymbol{K}$ is increased to a predetermined maximum value. The K-Best SD algorithm is summarized as follows.

Since complex signals (i.e. I and Q) are being processed, a real domain realization of the tree search results in a single $2N_t$-dimensional search (i.e. one for real and one for imaginary). The breadth first search begins with the N_t^{th} layer. For each nth layer, the algorithm computes the $\boldsymbol{K}$ best partial candidates $\left[\boldsymbol{s}_1^{(n)}, \boldsymbol{s}_2^{(n)}, \ldots, \boldsymbol{s}_K^{(n)}\right]$, where a partial candidate $\boldsymbol{s}_i^{(n)}$ represents the i^{th} path through the tree from the root node to level n, and is given by $\left[s_{i,n}^{(n)}, s_{i,n+1}^{n}, \ldots, s_{i,N_t}^{(n)}\right]^T$. The error at each step is measured by the partial Euclidean distance (PED), e.g. the accrued error at a given level of the tree, for a given path through the tree. Clearly, the $\boldsymbol{K}$ candidates at level n represent the $\boldsymbol{K}$ partial candidates with the minimum PED among all the children of the $\boldsymbol{K}$ candidates of the $(n+1)$-st level, where the distance is calculated via:

$$PED_i^{(n)} = \sum_{j=n}^{N_t}\left[\left(\tilde{y}_j - \sum_{k=j}^{N_t} R_{j,k} s_{i,k}^{(n)}\right)^2\right]. \qquad (4)$$

For an arbitrary level of the tree, the $\boldsymbol{K}$ best nodes are collected, and passed to the next level for consideration. In the last step the $\boldsymbol{K}$ paths through the tree are evaluated to determine the path with the minimum total error.

III. Prior Art

Previous published work describes both K-best and depth-first search SD algorithms for MIMO detection. In [7], authors present a 192Mbps 4x4 MIMO for IEEE 802.11n supporting 16-QAM OFDM using the V-BLAST algorithm. The work in [9] presents a 4x4 depth-first search SD detector that achieves 73Mbps and a slightly altered implementation using a modified Schnorr-Euchner (SE) enumeration scheme [8] which results in 170Mbps throughput. In [2], authors implement a K-best SD detector also using SE enumeration and modify it to support soft outputs, consuming 626mW at 100MHz, at 2.8V supply with throughput of 100Mbps. The most energy-efficient results published to date relating to SD detection are presented in [10] and [11] where a 16-core architecture using a hybrid K-best breadth-first, depth-first search approach results in a scalable MIMO detector supporting 2x2 to 8x8 configurations and BPSK to 64-QAM modulation schemes in 0.97mW for the hard-output SD kernel at a supply voltage of 0.42V and 10MHz frequency. More recent work published in [12] presents a non-deterministic depth-first SD decoder supporting up to 4x4 64-QAM MIMO, resulting in 335Mbps throughput.

The work presented in this paper distinguishes itself from previously published work in that our MIMO detector adapts its computation based on channel SNR conditions and application BER targets to reduce total energy and computational complexity. In our work, we implement a single detector that can approximate a linear detector when channel conditions are very good and a near-ML detector when channel conditions are poor.

IV. Channel-Adaptive K-Best Sphere Decoder

This section details the new MIMO detecting approach based on adaptation to channel conditions to achieve high energy-efficiency. Channel-adaptive K-best SD detection automatically adjusts computation to fluctuating factors in the MIMO channel, such as wide dynamic SNR range, different fading paths, and varying BER target requirements driven by applications or user experience. In contrast to previous solutions, we implement feedback from channel and CQI estimation (see Fig. 3) to adapt the K-best SD MIMO detector to reduce computation and power during favorable channel conditions and application BER targets. In previous publications, the number of search paths are fixed throughout the entire lifetime of the K-best SD detection.

In the LTE standard, the channel quality indicator CQI is a 4-bit value that the user equipment must estimate which indicates channel quality which is sent to the transmitter to adapt the modulation scheme to channel conditions to

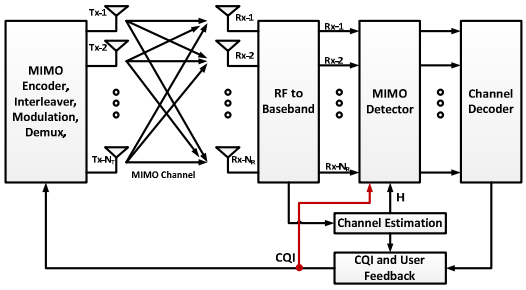

Figure 3. CQI feedback to channel-adaptive MIMO detector

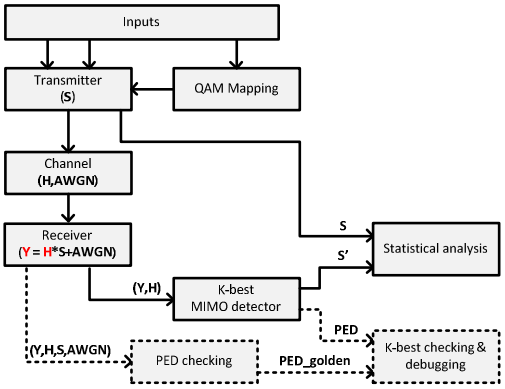

Figure 4. MATLAB model of channel-adaptive K-best MIMO detector

maximize channel efficiency [1]. Reference [1] provides more details on how the 4-bit CQI value is determined and how often it must be relayed to the transmitter. In this work we leverage the CQI so that we can dynamically vary $\boldsymbol{K}$ depending on channel quality as shown in Fig. 3. If $\boldsymbol{K}$ is arbitrarily large (e.g. to positive infinity), the search becomes exhaustive as in ML detection. If $\boldsymbol{K} = \mathbf{1}$, the detector reduces its computation to linear MMSE detection. Tuning $\boldsymbol{K}$ between these two extreme limits allows traversal of the BER vs. SNR vs. computational complexity tradeoff space as shown in Fig. 2.

The control algorithm adjusts the search radius $\boldsymbol{K}$ based on whether channel SNR meets certain threshold requirements. For example in a 4x4 16-QAM MIMO system, when the channel has high SNR (>25dB), then the search radius is set to $\boldsymbol{K} = \mathbf{1}$ and additional compute elements are power-gated off. In low SNR conditions (<10dB), the search radius is set to $\boldsymbol{K} = \mathbf{5}$ and all compute elements are active. The adaptive MIMO detector targets a maximum $\boldsymbol{K}$ (i.e., $\boldsymbol{K} = \mathbf{5}$) based on the worst-case channel response. Figure 4 shows the Matlab model for the K-best MIMO detector which is used to evaluate performance as shown in Fig. 5. The model allows users to change design parameters including size of the antenna array (e.g. 2x2, 2x4, 4x4, 8x8, and so on), the modulation scheme from BPSK to 256-QAM, and the search radius $\boldsymbol{K}$. Simulation results for a 4x4 MIMO system with 16-QAM modulation under a standard Rayleigh fading channel with white Gaussian noise (see Fig. 5) show that when $\boldsymbol{K} = \mathbf{1}$, the K-Best algorithm provides better performance than other common sub-optimum detectors, such as zero-forcing algorithm and

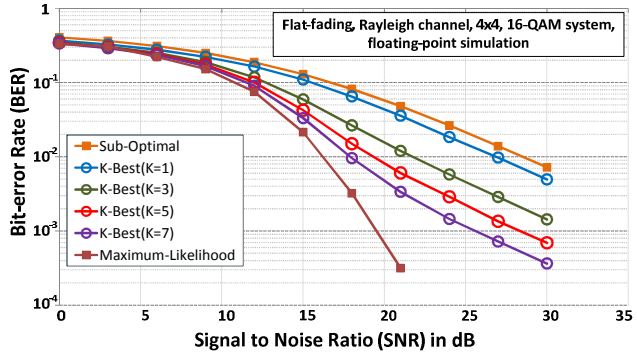

Figure 5. 4x4, 16-QAM K-Best MIMO Simulation

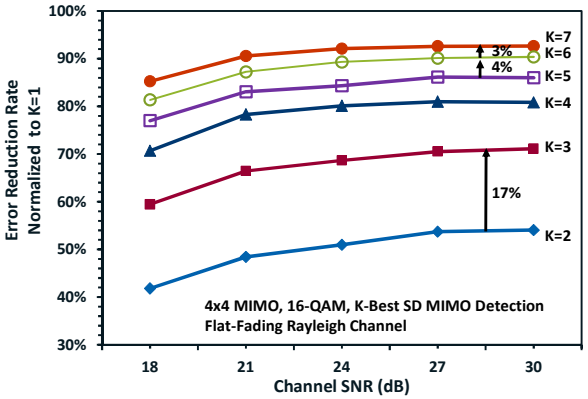

Figure 6. Error reduction rate for K-best MIMO

MMSE estimation. As shown in Fig. 6, when $\boldsymbol{K} > 5$, the incremental error reduction rate becomes marginal (<5%) for the K-best SD detector supporting up to 4x4, 16-QAM, indicating that near-optimum results are possible without exhaustive search. Hence, for the detector presented in this work, maximum $\boldsymbol{K}$ is chosen to be 5. The implementation is presented next.

V. Adaptive K-Best SD Detector Implementation

K-best SD MIMO detection is typically realized as a multi-stage pipeline since no trace-back is required. $\boldsymbol{K}$ paths through the search tree can be processed in parallel using a parallel architecture [10] and is typically fixed at some predetermined maximum $\boldsymbol{K}$. In contrast to other work, the MIMO detector presented here can vary $\boldsymbol{K}$ from 1 to 5 depending on channel SNR or CQI. This 8-stage channel-adaptive K-best SD detector is implemented in System Verilog and supports up to 4x4 antenna configuration and BPSK to 16-QAM modulation. The design is implemented in 22nm CMOS [13] and simulated for different configurations. An overview block diagram of the channel-adaptive K-best MIMO detector is shown in Fig. 7. The CQI indicates when to power-gate and clock-gate compute elements.

A single stage of the design consists of four main blocks: branch interference (BI) cancelation unit, a sorting circuit, storage of K-best candidates, and a merge unit. The details of these blocks are shown in Figure 8. The BI unit calculates the interference from detected signals on the symbol candidate and mitigates the interference. The sorting circuit sorts the potential symbol candidates based on an SE enumeration scheme and PED. The K-entry storage block stores the K-best candidates that have been found so far and

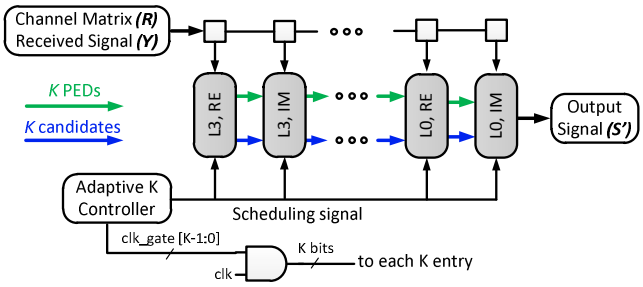

Figure 7. System overview of channel-adaptive K-best MIMO detector

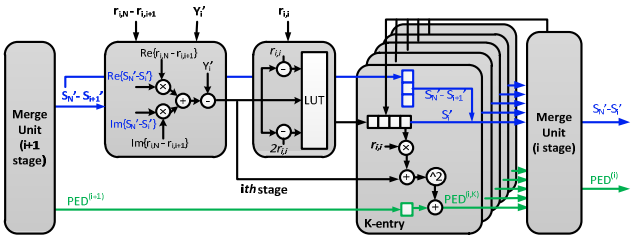

Figure 8. Detailed implementation of single stage

updates the PEDs for each of the candidate paths through the tree. The Merge Unit selects the K-best symbol candidates for each cycle based on the PEDs for the path traversed through the tree and propagates them to the next stage.

An adaptive-K control unit uses a simple look-up-table (LUT) based on the 4-bit CQI value to output power-gating and clock-gating scheduling signals such as clk_gate to turn off the K-entry storage blocks that are not required in good channel conditions. For example, if the CQI is between 1101 and 1111 (indicating good channel conditions), then clk_gate signal is 00001 indicating that $\boldsymbol{K = 1}$ and all but one of the K-entry storage blocks is required. The BI unit, the sorting circuit, the Merge Unit in each stage remain inactive for $(\boldsymbol{K_{max} - K})$ cycles when $\boldsymbol{K < K_{max}}$. These units are clock-gated off during inactive cycles. Using the same CQI signal as input to the MIMO detector creates closed-loop feedback inside the MIMO receiver as shown earlier in Figure 3.

Pipeline scheduling and time interleaving are implemented to eliminate stalls and improve throughput. Analysis shows that the K-entry block can introduce stalls and reduce the utilization of other three blocks if implemented without time-interleaving. To prevent the stalls, the K-entry block is doubled in size to accommodate time-interleaving.

VI. Simulation Results in 22nm CMOS

The configurable, channel-adaptive K-best SD MIMO detector, supporting up to 4x4 array configuration and modulation schemes up to 16-QAM, was simulated in 22nm Tri-gate CMOS [13] for area and power estimates at 1.0GHz target frequency and 0.80V supply voltage. The total power varies from 15mW ($\boldsymbol{K = 1}$) to 35mW ($\boldsymbol{K = 5}$) with energy-efficiency of 14.2pJ/bit ($\boldsymbol{K = 1}$) to 44.7pJ/bit ($\boldsymbol{K = 5}$). The latency per process array is dependent on $\boldsymbol{K}$ given by

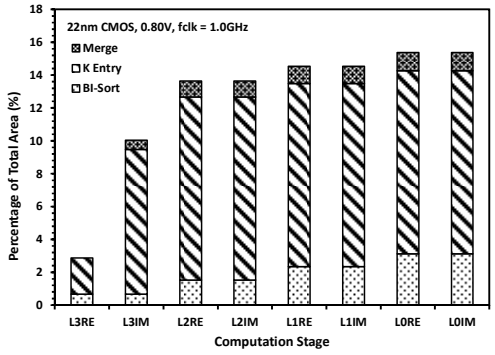

Figure 9. Percentage distribution of total area across computation stages.

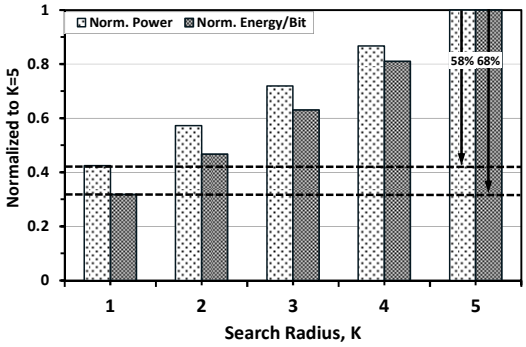

Figure 10. Effect of adapting $\boldsymbol{K}$ on power and energy efficiency

$\boldsymbol{(35 + 7 \times K)}$: 42 cycles when $\boldsymbol{K = 1}$ and 70 cycles when $\boldsymbol{K = 5}$. At 1.0GHz, the simulated throughput is 3.2Gbps.

The area distribution across stages and compute blocks is given in Fig. 9. The K-entry blocks across all stages consume 78% of the total area whereas the BI unit, sorting circuits, and merge units make up the rest of the area. A summary of the simulation results using default activity and input toggle factors is given in Table 2.

The effect of adapting $\boldsymbol{K}$ to channel conditions is shown in Figure 10. As $\boldsymbol{K}$ is reduced from 5 to 1, there is a 68% reduction in energy per bit and 58% reduction in total power. This simulation includes the reduced activity of blocks that are inactive when $\boldsymbol{K < K_{max}}$. When $\boldsymbol{K}$ is dynamically adjusted to provide a constant BER over a varying SNR conditions, gains in energy-efficiency are realized by tuning $\boldsymbol{K}$ to channel conditions as outlined in the next section.

Table 2. Summary of 22nm CMOS synthesis results

Detecting Method	Channel-Adaptive K-best SD
Technology	22nm CMOS, 0.80V
Clock frequency	1.0GHz
Latency (K=1 to K=5)	42 – 70 cycles
Total power (K=1 to K=5)	15.1 – 35.5 mW
Energy per bit (K=1 to K=5)	14.2 – 44.7 pJ/bit
Throughput	3.2Gbps

A. High BER Case Study

Consider a high BER application where the target BER is set to 10^{-1}. Assuming typical range of wireless received signal power is -70dBm to -90dBm and the thermal noise floor is set to -111dBm, we consider the 10dB to 30dB SNR range as shown in Fig. 11 which displays BER curves for the channel adaptive K-best MIMO detector operating with $\boldsymbol{K = 5}$ and $\boldsymbol{K = 1}$. At an SNR ≤15dB, we are forced to operate the detector with $\boldsymbol{K = 5}$, dissipating 44.7pJ/bit. When channel SNR is greater than15dB, $\boldsymbol{K}$ is adapted to one and energy dissipation reduces to 14.2pJ/bit, resulting in 51% energy savings assuming that channel SNR varies uniformly from 10dB to 30dB.

B. Low BER Case Study

Figure 12 shows an application with a target BER lower than 10^{-2}. In this case, when channel SNR is less than 21dB,

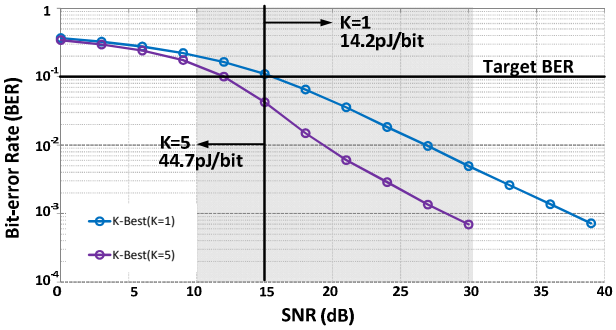

Figure 11. High BER application channel adaptation case study

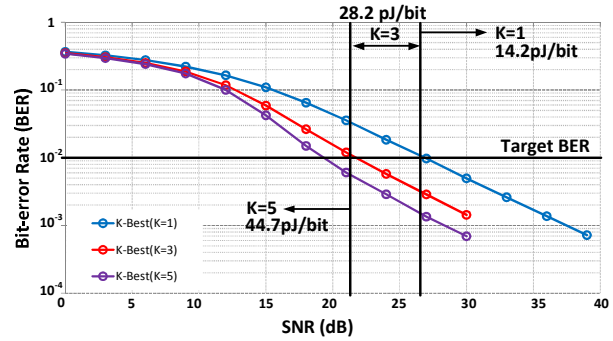

Figure 12. Low BER application channel adaptation case study

the MIMO detector must operate with $\boldsymbol{K = 5}$ to achieve the desired BER target. When channel conditions improve slightly (21dB < SNR ≤26dB) then $\boldsymbol{K}$ can be reduced to 3, resulting in 28.2pJ/bit energy dissipation. If the channel SNR improves such that SNR>26dB, then $\boldsymbol{K}$ can be reduced to 1. The total energy reduction in this case is 23% assuming channel SNR varies uniformly from 10dB to 30dB. Over a range of different target BER and channel conditions, an average of 10% to 51% energy reduction can be achieved using channel-adaptive K-best MIMO detection.

VII. Conclusions and Future Work

We have presented a unique approach to MIMO detection that uses channel information to adapt the search radius of a K-best SD detector, thereby enabling linear complexity in high SNR channel conditions, while maintaining BER performance during low SNR channel conditions. The estimated energy-reduction through simulations ranges from 10% to 51%, depending on target BER and channel SNR. During unfavorable SNR channel conditions, the MIMO detector satisfies the target BER by operating at $K = 5$. When channel SNR is high, 22nm circuit simulations demonstrate 68% reduction in energy-per-bit by setting $K = 1$, while maintaining target BER. The channel-adaptive MIMO detector achieves 3.2Gbps throughput at a target frequency of 1.0GHz at 0.80V supply and dissipates maximum 44.7pJ/bit when all compute elements are active.

In future, we plan to extend and optimize the channel-adaptive MIMO detector to support up to 8x8 array configurations and 64-QAM modulation schemes. We also plan to modify this architecture to support soft-output MIMO detection. In [14] the authors develop a method to modify a hard-output SD MIMO detector to include soft-outputs at an area overhead of 58%. In our proposed architecture we would also need to modify the number of times that a node is visited and the leaf enumeration procedure. As in [14] the PED calculation would remain the same and some small amount of additional memory would be required to track soft output metrics.

Acknowledgment

The authors thank R. Iyer, K. Stewart, V. De, R. Forand, G. Taylor, V. Ilderem, W. H. Wang, I. Perez-Gonzalez, R. Krishnamurthy, M. Jorgovanovic, M. Weiner, and G. Chen for encouragement and discussions.

References

[1] 3GPP standards website: www.3gpp.org

[2] Z. Guo and P. Nilsson, "Algorithm and implementation of the K-best sphere decoding for MIMO detection", *IEEE Journal on Selected Areas of Communications*, Vol. 24, No. 3, pp. 491-503, March 2006.

[3] T. D. Chiueh, P.Y. Tsai and I. W. Lai, *Baseband Receiver Design for Wireless MIMO-OFDM Communications 2nd Edition*, John Wiley and Sons, Singapore, 2012.

[4] M. Mahdavi and M. Shabany, "Novel MIMO Detection Algorithm for High-Order Constellations in the Complex Domain", in *IEEE Transactions on VLSI Systems*, Vol. 12, No. 5, May 2013.

[5] E. Agrell, T. Eirksson, A. Vardy, and K. Zeger, "Closest point search in lattices," *IEEE Trans. Inf. Theory,* vol. 48, no. 8, pp. 2201-2214, Aug. 2002.

[6] S. A. Laraway and B. Farhang-Boroujeny, "Implementation of a Markov Chain Monte Carlo Based Multiuser/MIMO Detector", in *IEEE Transactions on Circuits and Systems – I*, Vol. 56, No. 1, pp. 246-255, January 2009.

[7] D. Perels et. al., "ASIC Implementation of a MIMO-OFDM Transceiver for 192Mbps WLANs", in *ESSCIRC Digest of Technical Papers*, Grenoble, France, Sept. 2005.

[8] C. P. Schnorr and M. Euchner, "Lattice basis reduction: Improved practical algorithms and solving subset sum problems," *Math. Programming*, vol. 66, pp. 181–191, 1994.

[9] A. Burg et. al., "VLSI Implementation of MIMO Detection Using the Sphere Decoding Algorithm", in *IEEE Journal of Solid-State Circuits*, Vol. 40, No. 7, pp. 1566-1577, July 2005.

[10] C. H. Yang and D. Markovic, "A Flexible DSP Architecture for MIMO Sphere Decoding", in *IEEE Transactions on Circuits and Systems-I*, Vol. 56, No. 10, pp. 2301-2314, 2009.

[11] C. H. Yang, T. H. Yu, and D. Markovic, "A 5.8mW 3GPP-LTE Compliant 8x8 MIMO Sphere Decoder Chip with Soft-Outputs", in *Technical Digest of Technical Papers for IEEE 2010 Symposium on VLSI Circuits*, Hawaii USA, June 2010.

[12] M. Winter, "A 335Mb/s 3.9mm2 65nm CMOS Flexible MIMO Detection-Decoding Engine Achieving 4G Wireless Data Rates", in *2012 ISSCC Digest of Technical Papers*, San Francisco, USA. February 2012.

[13] C. H. Jan et. al., "A 22nm SoC Platform Technology Featuring 3-D Tri-Gate and High-k/Metal Gate, Optimized for Ultra Low Power, High Performance and High Density SoC Applications", in *Proceedings of IEDM*, pp. 4-7, 2012.

[14] C. Studer, A. Burg, and H. Bolcskei, "Soft-Output Sphere Decoding: Algorithms and VLSI Implementation", in *IEEE Journal of Selected Areas in Communications*, Vol. 26, No. 2, pp. 290-300, February 2008.